Chapter-2

SHEATH STRUCTURE WITH ELECTRON-INERTIA IN MAGNETIZED PLASMAS

Abstract: *The equilibrium properties of planar plasma sheath with electron-inertia in two-component magnetized bounded plasmas*[†] *is methodologically investigated. It is seen that the derived Bohm condition for the sheath formation is considerably modified (supercriticality), and so forth. A multi-parametric numerical analysis is provided to depict the new sheath features against the conventional ones (with inertialess electrons) alongside future scope.*

2.1 INTRODUCTION

It is a well-known fact that the bulk plasma (presheath) in any bounded plasma system is interactively coupled to the confining wall only via the process of sheath formation (indirect coupler). The terminology 'plasma sheath', 'sheath' or 'Debye sheath' is originally coined to represent a thin non-neutral space-charge layer (dark in colour) formed due to electrostatic polarization developed between the bulk plasma (system size order) and the absorbing wall [1-4]. The bounded plasma indeed shields itself from the resulting electric field (due to loss of lighter, more mobile electrons to the wall) by means of the sheath-creation (positive charge region, Debye length order). The threshold value of the ion flow at the sheath entrance is given by a well-established (local) condition known as the Bohm criterion [2-8].

The existence of plasma sheath can naturalistically be realized in a wide-range domain of scales from laboratories to galaxies. The principal importance of sheath physics here is due to various technological applications, such as the Langmuir probe diagnostics, mass-spectrometry, plasma-wall interactions in thermonuclear fusion devices, plasma processing of materials, Hall thrusters, energy-harvesting reactors, and so forth [5-8].

In this chapter, we herein present a hydrodynamic (bi-fluidic) model to study the *Bohm criterion* in two-component magnetized plasma in the presence of active electron-

[†]Gohain, M. and Karmakar, P. K. Evolutionary sheath structure in magnetized collisionless plasma with electron inertia. *Plasma Physics Reports*, 43(9):957-968, 2017.

inertial role. Both the constituent electrons and ions are taken to be magnetized in the presence of an oblique (relative to the bulk fluid flow) magnetic field. In our model, the relevant physical parameters (density, potential and velocity) vary only in a direction normal to the confining wall boundary [9]. A new construct of the Bohm criterion is derived and established. The new sheath evolutionary dynamics resulting from the consideration of non-trivial electron-inertial effects is investigated illustratively alongside anticipated future scope.

2.2 PLASMA MODEL AND FORMALISM

A hydrodynamic model of magnetized quasi-neutral collisionless plasma in a planar (flat) geometry configuration is considered. The model consists of hydrogenic ions (H^+, inertial species) and tiny electrons (e^-, thermal species) coupled via ambipolar polarization effects. The presence of neutrals and other impurity ions is ignored for simplicity. The adopted model highlights the lowest-order electron-inertial correction (fluid, modified Boltzmann) over its leading-order distribution (inertialess, pure Boltzmann) [6-12]. The justification for the electron-inertia is attributable to the unstable transonic plasma zone (between bulk and sheath). It is rich in random acoustic fluctuations unshielded by inertial electrons [10-11].

The schematic diagram of magnetized plasma sheath configuration, where the external magnetic field acts in the $(x-z)$ plane, at a directional angle θ with respect to the bulk plasma flow (along the *x*-axis) is depicted in figure 2.1. At the sheath edge (sheath-presheath boundary), $x=\lambda_{De}\xi=0$ and $\phi=-(T_e/e)\Phi=0$. Again, at the wall, $x_w=\lambda_{De}\xi_w$ and $\phi=-(T_e/e)\Phi_w\neq 0$. Here, ξ is the normalized space coordinate and Φ is the normalized electrostatic potential (normalization defined later).

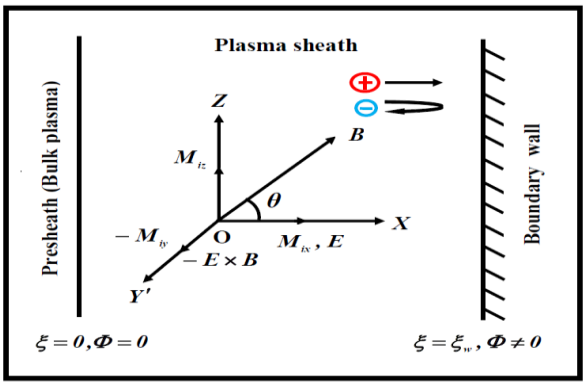

Figure 2.1: *Schematic diagram of the considered magnetized plasma sheath configuration.*

It may be now pertinent to give a rough idea about the fundamental relevant properties of the model setup. The estimation is carried out in the usual plasma parametric domain [13-15]. The magnitude of electronic (protonic) charge is $e = 1.6\times10^{-19}$ C; electronic mass, $m_e = 9.1\times10^{-31}$ kg; and ionic (protonic) mass, $m_i = 1.67\times10^{-27}$ kg. The external magnetic field is B = 0.1 T; and electron-to-ion temperature ratio, $\sigma = T_e/T_i = 1$. The estimated value of electron cyclotron frequency is $\omega_{ce} = eB/m_e \approx 1.75\times10^{10}$ rad sec^{-1} and that of ion cyclotron frequency is $\omega_{ci} = eB/m_i \approx 9.58\times10^{6}$ rad sec^{-1}. Therefore, the ratio of electron-to-ion cyclotron frequencies roughly comes out as $\omega_{ce}/\omega_{ci} = m_i/m_e \approx 1.83\times10^{3}$. Similarly, the electron gyro radius is $r_{ge} = m_e v_e/eB \approx 2.38\times10^{-5}$ m, and the ion gyro radius is $r_{gi} = m_i v_i/eB \approx 1.02\times10^{-3}$ m. Hence, the electron-to-ion gyration radii ratio is $r_{ge}/r_{gi} = \sqrt{\sigma}\times\sqrt{m_e/m_i} \approx 2.3\times10^{-2}$. The estimation indicates that both the electronic and ionic dynamics are sensible to the magnetic field. Eventually, we adopt both electrons and ions magnetized; instead of unmagnetized electrons, against traditional viewpoints [16-19].

The evolutionary set of the structuring equations in time-stationary form with all the customary notations in dimensional form [20] is constructed as follows. The zeroth-order electronic dynamics with zero-inertia ($m_e/m_i \to 0$) is described with the Boltzmann law as

$$n_e = n_0 \exp\left(\frac{e\phi}{T_e}\right), \tag{2.1}$$

where, ϕ is the self-consistent electrostatic potential and T_e is the electron temperature (in eV). The goal here is to incorporate the weak but finite electron-inertia over the leading-order (equation (2.1)). The corresponding electron continuity and momentum equations in the steady-state ($\partial/\partial t \sim 0$) in the leading-order are respectively given as

$$\vec{\nabla}.(n_e \vec{v_e}) = 0, \tag{2.2}$$

$$-en_e\vec{E} - T_e\vec{\nabla}n_e - e(\vec{v_e}\times\vec{B}) = 0. \tag{2.3}$$

Based on the existing literature regarding inclusion of the weak but finite electron-inertial effects in a compatible procedural way [8, 10-12], equation (2.3) in the presence of weak but finite electron-inertia can also be presented as follows

$$m_e n_e\left[\left(\vec{v}_e.\vec{\nabla}\right)\vec{v}_e\right]=-en_e\vec{E}-T_e\vec{\nabla}n_e-e(\vec{v}_e\times\vec{B}). \tag{2.4}$$

The methodological details on simultaneous application of the Boltzmann distribution law (leading-order solution on density with zero-inertia) and hydrodynamic equations (inertially perturbed solution on the lowest-order inertia) to incorporate the weak but finite electron-inertia have already been established in the past [8, 10-12].

The different notations n_e, m_e, v_e, e and E represent the number density, inertial mass, flow velocity, electric charge of the electrons; and the self-consistent electric field; respectively. Similarly, the steady-state ion fluid continuity and momentum equations under the isothermal pressure, $p_i=\gamma T_i n_i$, are respectively presented as

$$\vec{\nabla}.(n_i\vec{v}_i)=0\ , \tag{2.5}$$

$$(\vec{v}_i.\vec{\nabla})\vec{v}_i=-\frac{e}{m_i}\vec{\nabla}\phi+\frac{e}{m_i}(\vec{v}_i\times\vec{B})-\frac{1}{m_i n_i}\vec{\nabla}p_i\ . \tag{2.6}$$

Lastly, the electrostatic Poisson equation coupling the electron-ion dynamics is given by

$$\nabla^2\phi=-\frac{e}{\in_0}(n_i-n_e)\ . \tag{2.7}$$

The relevant physical parameters (plasma density, electrostatic potential and flow velocity) are assumed to vary only in a direction normal to the confining wall boundary. It implies that the parameters vary only in the *x*-direction, for which $\vec{\nabla}\to\hat{x}\partial/\partial x$, and the *B*-direction is $\hat{B}=\hat{x}\cos\theta+\hat{z}\sin\theta$, where θ is the *B*-obliquity relative to the bulk flow. In such a case, the *z*-component of the ionic dynamics is ignorable. So, the basic set of governing equations (from equations (2.1)-(2.7)) dictating the *x*-directional dynamics can respectively be written as

$$n_e=n_0\exp\left(\frac{e\phi}{T_e}\right), \tag{2.8}$$

$$\frac{\partial}{\partial x}(n_e v_e)=0\ , \tag{2.9}$$

$$m_e n_e\left(v_{ex}\frac{\partial v_{ex}}{\partial x}\right)=en_e\frac{\partial\phi}{\partial x}-T_e\frac{\partial n_e}{\partial x}-e\,v_{ey}B\sin\theta\ , \tag{2.10}$$

$$\frac{\partial}{\partial x}(n_i v_i) = 0 \ , \tag{2.11}$$

$$v_{ix}\frac{\partial v_{ix}}{\partial x} = -\frac{e}{m_i}\frac{\partial \phi}{\partial x} + \frac{e}{m_i}v_{iy}B\sin\theta - \frac{1}{m_i n_i}\gamma T_i \frac{\partial n_i}{\partial x} \ , \tag{2.12}$$

$$\frac{\partial^2}{\partial x^2}(\phi) = -\frac{e}{\in_0}(n_i - n_e) \ . \tag{2.13}$$

In order to see the scale-invariant sheath features, we present the customary normalization procedure, as shown in Table 2.1.

Table 2.1: Adopted normalization scheme

S No.	Physical parameters	Normalizing parameters	Typical value
1	Position (ξ)	Plasma Debye length	$\lambda_{De} \approx 3.32\times10^{-4}$ m [27]
2	Population density (N_e, N_i)	Equilibrium density	$n_0 \approx 5\times10^{14}$ m^{-3} [27]
3	Mach number (M_e, M_i)	Sound phase speed	$c_s \approx 1\times10^{4}$ m s^{-1} [27]
4	Electric potential (Φ)	Plasma thermal potential	$T_e/e \approx 1$ J C^{-1} [27]

The ion acoustic phase speed, in the usual notations and units [20], is given by $c_s = \sqrt{(T_e + \gamma T_i)/m_i}$, with γ =1 for the isothermal ionic fluid. The normalized form of equations (2.8)-(2.13) is respectively constructed and cast as

$$N_e = \exp(-\Phi), \tag{2.14}$$

$$\frac{\partial}{\partial \xi}(N_e M_e) = 0 \ , \tag{2.15}$$

$$\left(\frac{m_e}{m_i}\right)M_e\left(\frac{\partial M_e}{\partial \xi}\right) = -\frac{\partial \Phi}{\partial \xi} - \frac{1}{N_e}\frac{\partial N_e}{\partial \xi} - \frac{1}{N_e}\left(\frac{1}{n_0}M_{ey}\alpha\sin\theta\right). \tag{2.16}$$

It is seen here that only the last term on the right hand side of equation (2.16), $Y_L = \left\lfloor 1/N_e\left((1/n_0)M_{ey}\alpha\sin\theta\right)\right\rfloor$, represents a cross-coupling parametric term mapping

orthogonal interaction of the electron population (N_e evolving along $\hat{x}$) with its flow (M_{ey} evolving along $\hat{y}$). Here, $\alpha = \omega_{ci}/\omega_{pi}$ is the ratio of the ion cyclotron frequency $\omega_{ci} = eB/m_i$ to the ion plasma frequency $\omega_{pi} = \sqrt{n_0 e^2/\in_0 m_i}$. In order for simplification to our *x*-directional planar problem, let us first examine its relative strength. We now, for estimation, adopt a plasma parametric window [8, 18] as $M_{ey} = 10^{-1}$, $B =$ 0.1 T, $n_0 = 5\times10^{14}$ m^{-3}, $\in_0 = 8.854\times10^{-12}$ F m^{-1} and $\theta = 30^0$. Clearly, our estimation further shows that $\alpha = \sqrt{\in_o B^2/n_o m_i} \sim 3.16\times10^{-1}$. In such a situation, we estimate the term strength as $Y_L \sim 10^{-18}\left(1/N_e\right)$. It indicates insignificant Y_L-effects in the electronic dynamics on the laboratory scales of space and time. Thus, equation (2.16) justifiably simplifies to

$$\left(\frac{m_e}{m_i}\right) M_e \left(\frac{\partial M_e}{\partial \xi}\right) = -\frac{\partial \Phi}{\partial \xi} - \frac{1}{N_e}\frac{\partial N_e}{\partial \xi} \quad , \tag{2.17}$$

$$N_i M_{ix} = M_{i0} , \tag{2.18}$$

$$M_{ix}\frac{\partial M_{ix}}{\partial \xi} = \frac{\partial \Phi}{\partial \xi} + M_{iy}\alpha \sin\theta - \frac{\gamma}{\sigma}\frac{1}{N_i}\frac{\partial N_i}{\partial \xi} , \tag{2.19}$$

$$\frac{\partial^2 \Phi}{\partial \xi^2} = N_i - N_e . \tag{2.20}$$

Here, $\sigma = T_e/T_i$ is the electron-to-ion temperature ratio (both in eV). Coupling equation (2.14) with equations (2.15) and (2.17), the inertia-corrected electron distribution becomes

$$N_e = \exp\left[\frac{1}{2}\left(\frac{m_e}{m_i}\right) M_{e0}^2 \left(1 - e^{2\Phi}\right) - \Phi\right], \tag{2.21}$$

which, on the Φ-differentiation once, yields

$$\frac{\partial N_e}{\partial \Phi} = -\exp\left[\frac{1}{2}\left(\frac{m_e}{m_i}\right) M_{e0}^2 \left(1 - e^{2\Phi}\right) - \Phi\right]\left[1 + \left(\frac{m_e}{m_i}\right) M_{e0}^2 e^{2\Phi}\right]. \tag{2.22}$$

Now, using $M_{ix} = M_{io}/N_i$ from equation (2.18) in equation (2.19), we have

$$M_{iy}\alpha \sin\theta = -\frac{M_{i0}^2}{N_i^3}\frac{\partial N_i}{\partial \xi} + \frac{M_{i0}}{N_i^2}\frac{\partial M_{i0}}{\partial \xi} - \frac{\partial \Phi}{\partial \xi} + \frac{\gamma}{\sigma}\frac{1}{N_i}\frac{\partial N_i}{\partial \xi} \quad . \tag{2.23}$$

Multiplying both sides of equation (2.23) by $\left(\partial\Phi/\partial\xi\right)^{-1}$ and simplifying, we obtain

$$\frac{\partial N_i}{\partial \Phi} = -\left[1 + M_{iy}\alpha \sin\theta \left\{\frac{\partial \Phi}{\partial \xi}\right\}^{-1}\right]\left\{\left(\frac{M_{i0}^2}{N_i^3} - \frac{\gamma}{\sigma}\frac{1}{N_i}\right)^{-1}\right\}. \tag{2.24}$$

Differentiating equation (2.20) with respect to Φ; and substituting $\partial N_e/\partial\Phi$ and $\partial N_i/\partial\Phi$ from equations (2.22) and (2.24); respectively, one finds

$$\begin{aligned}\frac{\partial}{\partial \Phi}\left(\frac{\partial^2 \Phi}{\partial \xi^2}\right) &= -\left[1 + M_{iy}\alpha \sin\theta \left\{\frac{\partial \Phi}{\partial \xi}\right\}^{-1}\right]\left\{\left(\frac{M_{i0}^2}{N_i^3} - \frac{\gamma}{\sigma}\frac{1}{N_i}\right)^{-1}\right\} \\ &+ \exp\left[\frac{1}{2}\left(\frac{m_e}{m_i}\right)M_{e0}^2\left(1 - e^{2\Phi}\right) - \Phi\right]\left[1 + \left(\frac{m_e}{m_i}\right)M_{e0}^2 e^{2\Phi}\right].\end{aligned} \tag{2.25}$$

The integration of equation (2.25) with respect to Φ results in

$$\left(\frac{\partial^2 \Phi}{\partial \xi^2}\right) = -\int \left[\begin{aligned}&\left[1 + M_{iy}\alpha \sin\theta \left\{\frac{\partial \Phi}{\partial \xi}\right\}^{-1}\right]\left\{\left(\frac{M_{i0}^2}{N_i^3} - \frac{\gamma}{\sigma}\frac{1}{N_i}\right)^{-1}\right\} \\ &- \exp\left[\frac{1}{2}\left(\frac{m_e}{m_i}\right)M_{e0}^2\left(1 - e^{2\Phi}\right) - \Phi\right]\left[1 + \left(\frac{m_e}{m_i}\right)M_{e0}^2 e^{2\Phi}\right]\end{aligned}\right]\partial\Phi. \tag{2.26}$$

For smooth, nonoscillatory and monotonic transition of the plasma from presheath to sheath region via thin patching transonic plasma layer (as per the universal energy conservation rule), $\Phi = (-e\phi/T_e)$ should be minimum at the sheath edge [21]. Thus, for $\Phi = \Phi_{\min}$, the following derivative condition in terms of potential curvature needs to be fulfilled

$$\left(\frac{\partial^2 \Phi}{\partial \xi^2}\right) \geq 0\ . \tag{2.27}$$

Therefore, from equation (2.26), one gets

$$-\int \left[\begin{aligned}&\left[1 + M_{iy}\alpha \sin\theta \left\{\frac{\partial \Phi}{\partial \xi}\right\}^{-1}\right]\left\{\left(\frac{M_{i0}^2}{N_i^3} - \frac{\gamma}{\sigma}\frac{1}{N_i}\right)^{-1}\right\} \\ &- \exp\left[\frac{1}{2}\left(\frac{m_e}{m_i}\right)M_{e0}^2\left(1 - e^{2\Phi}\right) - \Phi\right]\left[1 + \left(\frac{m_e}{m_i}\right)M_{e0}^2 e^{2\Phi}\right]\end{aligned}\right]\partial\Phi \geq 0, \tag{2.28}$$

Equation (2.28), after the Φ-differentiation on both sides, yields

$$-\frac{\partial}{\partial\Phi}\int \left[\begin{aligned}&\left[1 + M_{iy}\alpha \sin\theta \left\{\frac{\partial \Phi}{\partial \xi}\right\}^{-1}\right]\left\{\left(\frac{M_{i0}^2}{N_i^3} - \frac{\gamma}{\sigma}\frac{1}{N_i}\right)^{-1}\right\} \\ &- \exp\left[\frac{1}{2}\left(\frac{m_e}{m_i}\right)M_{e0}^2\left(1 - e^{2\Phi}\right) - \Phi\right]\left[1 + \left(\frac{m_e}{m_i}\right)M_{e0}^2 e^{2\Phi}\right]\end{aligned}\right]\partial\Phi \geq 0\ . \tag{2.29}$$

Therefore, according to standard rules of basic integration [22], equation (2.29) gives

$$-\left[1+M_{iy}\alpha\sin\theta\left\{\frac{\partial\Phi}{\partial\xi}\right\}^{-1}\right]\left\{\left(\frac{M_{i0}^2}{N_i^3}-\frac{\gamma}{\sigma}\frac{1}{N_i}\right)^{-1}\right\}$$
$$+\exp\left[\frac{1}{2}\left(\frac{m_e}{m_i}\right)M_{e0}^2\left(1-e^{2\Phi}\right)-\Phi\right]\left[1+\left(\frac{m_e}{m_i}\right)M_{e0}^2e^{2\Phi}\right]\geq 0\,. \tag{2.30}$$

The boundary conditions, $\Phi\to 0$, $N_i\to 1$ and $\partial\Phi/\partial\xi\neq 0$, hold good at the sheath entrance point [18]. Applying the condition for monotonic plasma transition together with the proper boundary conditions, the local Bohm criterion is derived as

$$M_{i0}\geq\left[\left\{1+M_{iy}\alpha\sin\theta\left(\frac{\partial\Phi}{\partial\xi}\right)_{\Phi=0}^{-1}\right\}\left\{1-\left(\frac{m_e}{m_i}\right)M_{e0}^2\right\}+\left(\frac{\gamma}{\sigma}\right)\right]^{1/2}, \tag{2.31}$$

where, as already indicated, $M_{i0}=v_{ix0}/c_s$ is the ion Mach number at $\xi\approx 0$. It is seen that the ion Mach threshold value gets drastically modified due to the presence of lowest-order electron-inertial correction (m_e/m_i), magnetic field (B) and the thermal motion of the ions ($\sigma=T_e/T_i$). It may be noted that the above inequality holds good only when the degree of ion-neutral collision is too small to affect the collective plasma dynamics.

2.3 RESULTS AND DISCUSSIONS

The analytical formalism for the magnetized collisionless plasma sheath structure in the presence of electron-inertia is now established. The non-trivial findings of applied value obtained from our simplified calculation schemes on are discussed below.

2.3.1 ANALYTICAL RESULTS

The analytical model to study the time-stationary sheath structure formation in the presence of both the Lorentz force and active electron-inertial dynamics on the lowest-order is methodologically constructed. The magnetic field acts at an oblique angle relative to the background ion flow. The local Bohm criterion for sheath formation is obtained systematically. The inclusion of the electron-inertia in association with the Lorentz gyro-kinetic effects is analytically found to play a crucial role in influencing the sheath

characteristics. It is found that the threshold value of the ion Mach number (M_{i0}) entering the sheath edge layer is slightly enhanced. For the different parameter values [23, 24] like $M_{iy}=10^{-2}$, $B=0.1$ T, $n_0=5\times10^{14}$ m^{-3}, $\theta=30^0$, $M_{e0}=1$, $\gamma=1$, $\sigma=T_e/T_i=3.33$ and $(\partial\Phi/\partial\xi)_{\Phi=0}=0.01$, one finds $M_{i0}\geq1.139$. This is a first consequence of the considered factors in our analysis against the conventional picture of $M_{i0}\geq1.139$.

2.3.2 NUMERICAL RESULTS

The basic governing equations for modelling plasma sheath structurization are now constructed. A numerical illustrative analysis to see the sheath evolutionary characteristics is carried with the help of fourth-order Runge-Kutta (RK-IV) method [25], as an initial value problem (IVP), to produce the numerical profiles as shown below.

Figure 2.2 illustrates the spatial profiles of the normalized (a) electron and ion population densities (N_e and N_i), (b) ion-flow velocity (M_i), (c) electrostatic potential (Φ), and (d) electrostatic potential curvature ($\partial^2\Phi/\partial\xi^2$) under different strengths of the applied magnetic field ($B=0.1$, 0.2 and 0.3 T). The different input initial values [15, 20] used are $\xi_i=0.01$ with $\Delta\xi=$ 0.01, $N_{e0}=1$, $N_{i0}=1$, $M_{ix0}=10^{-1}$, $(\Phi)_i=-1\times10^{-2}$ and $(\Phi_{\xi\xi})_i=-1\times10^{-3}$; respectively. The fixed input parameters [8, 18, 20] are $M_{e0}=1$, $M_{i0}=1$, $M_{iy0}=10^{-2}$, $n_0=5\times10^{14}$ m^{-3}, $\alpha=3.20\times10^{-1}$, $\gamma=1$, $\sigma=1$ eV, and $\theta=30^0$.

It is seen that N_e and N_i go on decreasing with increase in the *B*-value [figure 2.2(a)]. The deviation from quasi-neutrality increases with increase in *B*. This is because of enhanced ion gyro-kinetic effects. It confirms that the plasma sheath structure, so formed in our proposed model, is indeed a non-neutral (ion-rich) space-charge layer. It is further seen that, with the *B*-increment, M_i increases; and vice-versa [figure 2.2(b)]. It is because of the fact that, the ions get an additional boost because of the Lorentz force, the effect of which is more pronounced for stronger magnetic fields; and vice-versa, on the ion flow dynamics.

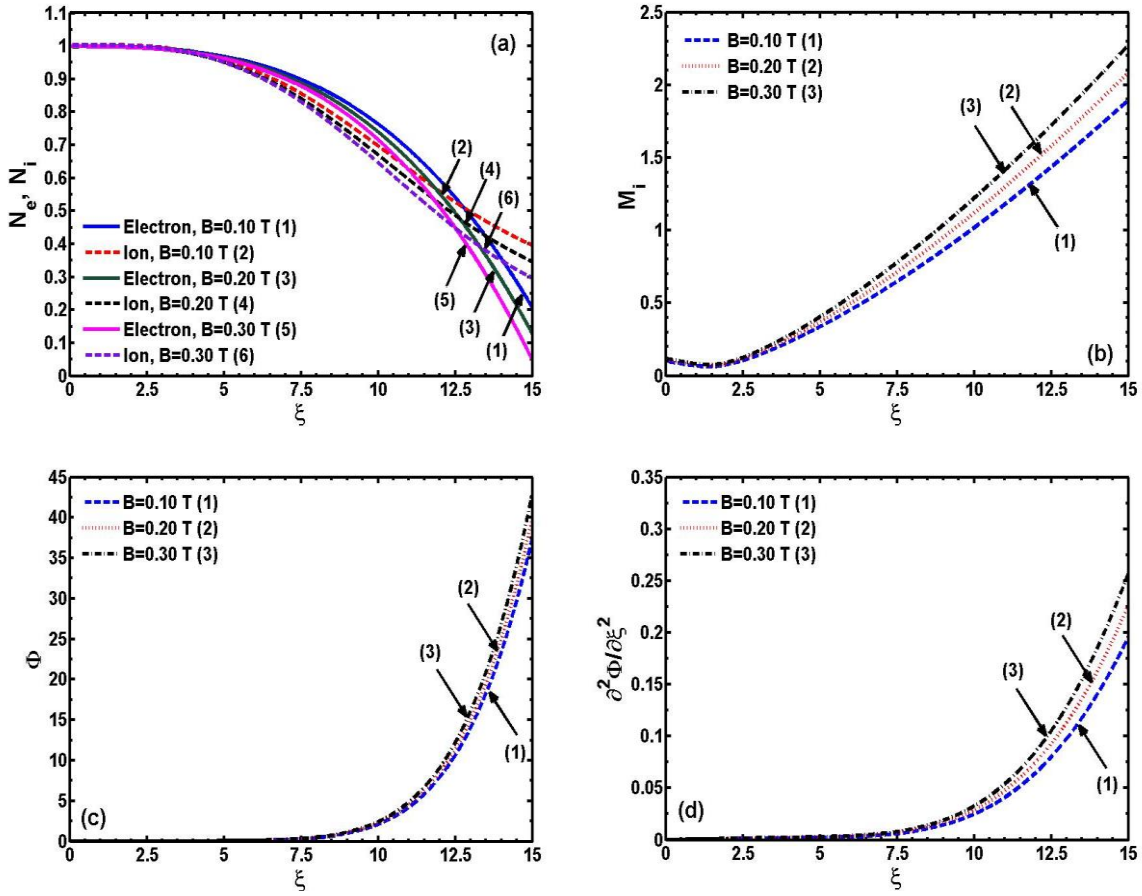

Figure 2.2: *The spatial profiles of the normalized (a) electron and ion population densities (N_e and N_i), (b) ion Mach number (M_i), (c) electrostatic potential (Φ), and (d) potential curvature ($\partial^2\Phi/\partial\xi^2$) under different strengths of the applied magnetic field (B). The two distinct line sets (solid and dashed) in figure 2.2(a) depict the electron and ion densities for $B = 0.1$ T, 0.2 T, and 0.3 T; respectively. The blue, red and black distinct lines in figures 2.2(b)-2.2(d) link to the same respective B-values. Fine details are given in the text.*

Figure 2.2(c) portrays the Φ-evolution under different *B*-values. It is realized that *B* plays an important role in holding up the ions gyro-kinetically in reaching the sheath region. The gyro-kinetic influence is more for larger *B*; and vice-versa. The electron-ion density separation is evident from the potential curvature [figure 2.2(d)]. It is seen that, with the *B*-increment, the deviation from quasi-neutrality increases thereby showing the non-neutral nature of the sheath structure.

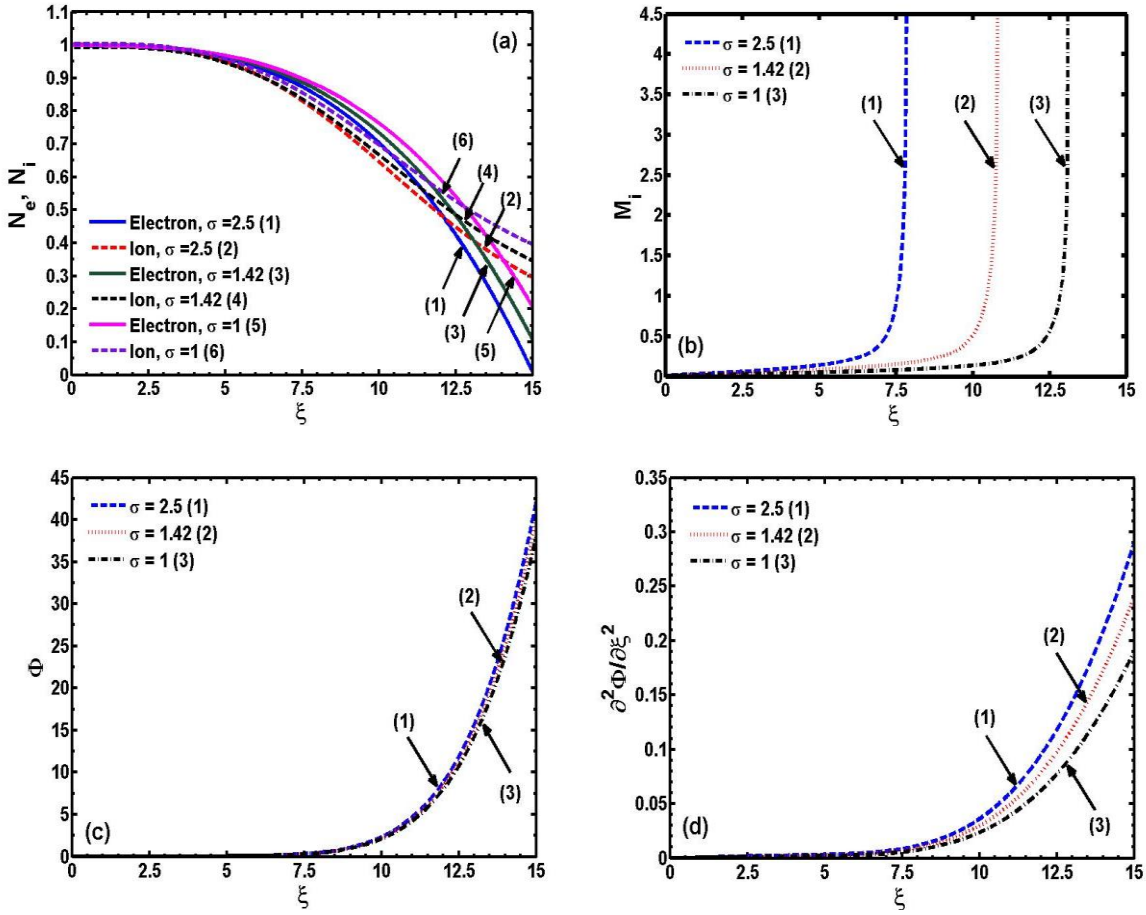

Figure 2.3: *Same as figure 2.2, but with* $B = 0.1$ *T and* $\theta = 30^0$. *Different lines link to* $\sigma = (T_e/T_i)$ *=2.5, 1.42, and 1; respectively. Here,* $T_e = 1$ *eV (fixed), and different* $T_i = 0.4$ *eV,* $T_i = 0.7$ *eV, and* $T_i = 1$ *eV; respectively.*

Figure 2.3 displays the same as in figure 2.2, but with $B = 0.1$ T and $\theta = 30^0$. Different lines now indicate $\sigma = (T_e/T_i) =$ 2.5, 1.42, and 1; respectively. Here, $T_e = 1$ eV (fixed), and different $T_i = 0.4$ eV, $T_i = 0.7$ eV, and $T_i = 1$ eV; respectively. Such situations are practically realizable in the magnetic confinement fusion plasmas and so forth [20]. It is seen that with increase in T_i-values, the deviation from quasi-neutrality decreases towards the sheath [figure 2.3(a), 2.3(d)]; and vice-versa. This is because with the T_i-increment, the random kinetic energy of the ions increases thereby getting enhanced flow speed. The degree of local charge-imbalance between the hetero-polar plasma species in the presence of B decreases. Thus, the ionic gyro-kinetic effects in association with the electrons, in turn,

decrease the electrostatic polarization potential (sheath potential) via the transonic equilibrium point. As a result, the sheath-width decreases slightly. This is interestingly a new original outcome due to the consideration of weak but finite electron-inertia under the action of the Lorentz gyro-kinetic effect in contrast with the previous predictions [23, 26].

Also, the *M*-profile [figure 2.3(b)] is found to be different in contrast with the other case as already discussed [figure 2.2(b)]. We infer that the T_i -increment slightly shifts the sonic point towards the sheath termination relative to the edge. In contrast, the variation in Φ [figure 2.2(c)] evolves quite well in comparison with the investigations by others [15].

2.3.3 COMPARATIVE RESULTS

The results investigated here are widely compared and discussed in the light of different existing scenarios [8, 18, 21, 24]. The following special cases derivable from the modified Bohm criterion obtained by us herein may also be worth mentioning.

Case (a)-Unmagnetized cold plasma in absence of electron-inertia:

Substituting $\alpha = 0$, $m_e/m_i \to 0$ and $T_i/T_e = 0$, in equation (2.31), one gets

$$M_{i0} \geq 1, \tag{2.32}$$

which is the well-established usual Bohm criterion [7, 21].

Case (b)-Unmagnetized cold plasma in presence of electron-inertia:

Substituting $\alpha = 0$ and $T_i/T_e = 0$, in equation (2.31), we have

$$M_{i0} \geq \left[\left\{ 1 - \left(\frac{m_e}{m_i} \right) M_{e0}^2 \right\} \right]^{1/2}. \tag{2.33}$$

The above inequation exactly matches with the Bohm criterion derived by Deka et al. [8].

Case (c)-Unmagnetized warm plasma without electron-inertia:

Substituting $\alpha = 0$, and $m_e/m_i \to 0$, in equation (2.31), one obtains

$$M_{i0} \geq \sqrt{1+1/\sigma}\,. \tag{2.34}$$

This inequation again matches with the analytical form of the local Bohm criterion as derived by Ghomi et al. [24], where $T = 1/\sigma = T_i/T_e$.

Case (d)-Magnetized cold plasma with no electron-inertia:

Substituting $T_i/T_e = 0$ and $m_e/m_i \to 0$, in equation (2.31), we get

$$M_{i0} \geq \left[\left\{ 1 + M_{iy}\alpha \sin\theta \left(\frac{\partial \Phi}{\partial \xi} \right)^{-1}_{\Phi=0} \right\} \right]^{1/2}, \tag{2.35}$$

which matches with the Bohm criteria as derived by Zou et al. [18].

Case (e)-Magnetized warm plasma without electron-inertia:

Substituting $m_e/m_i \to 0$, equation (2.31) gets modified to

$$M_{i0} \geq \left[\left\{ -M_{iy}\alpha \sin\theta \left(\frac{\partial \Phi}{\partial \xi} \right)^{-1}_{\Phi=0} \right\} \left\{ 1 + \left(\frac{\gamma}{\sigma} \right) \right\} \right]^{1/2}, \tag{2.36}$$

which matches with that by Ou et al. [20] after neglecting the collisional effects.

Case (f)-Magnetized warm plasma in presence of electron-inertia:

$$M_{i0} \geq \left[\left\{ 1 + M_{iy}\alpha \sin\theta \left(\frac{\partial \Phi}{\partial \xi} \right)^{-1}_{\Phi=0} \right\} \left\{ 1 - \left(\frac{m_e}{m_i} \right) M_{e0}^2 \right\} + \left(\frac{\gamma}{\sigma} \right) \right]^{1/2}, \tag{2.37}$$

which is the work on the modified Bohm threshold condition on the ion flow dynamics towards the sheath as proposed herein for the first time.

2.4 CONCLUSIONS

A collisionless bi-fluidic theoretical model is methodically developed to investigate the equilibrium structural features of steady-state plasma sheath in the presence of weak electron-inertia in magnetized plasma configuration. The local Bohm condition is found to be significantly influenced by the electron-inertial correction, applied magnetic field and its orientation relative to the bulk-flow. It is interestingly found that the threshold value of the ion flow entering the sheath edge is enhanced (typically, $M_{i0} \geq 1.139$, in normal plasma conditions [23, 24]) due to collective cooperative gyro-kinetic effects. A numerical illustrative platform shows that the relevant sheath characteristics get considerably modified due to the considered factors. The obtained results are compared and discussed in the panoptic light of the literature. To sum up, the following concluding remarks are in order.

1. The Bohm criterion for sheath formation in quasi-neutral collisionless plasma in an applied oblique magnetic field in the presence of active electron-inertial dynamics is analyzed.
2. The inclusion of electron-inertia, alongside the Lorentz gyro-kinetic effects, enhances the threshold ion Mach number towards the sheath entrance due to electron-inertial delay effect.
3. It is seen that the electron and ion densities decrease; ion flow velocity, potential and curvature increase with the increment of the applied magnetic field; and vice-versa.
4. The electron and ion densities increase; ion flow velocity slightly shifts the sonic point towards the sheath termination point relative to the sheath edge; potential and curvature decrease with increase in ion temperature; and vice-versa.
5. The quasi-neutrality breaks down, as the sheath edge is reached, with increase in the magnetic field strength. In contrast, the deviation from quasi-neutrality (indicated by potential curvature) decreases with increase in the ion temperature.

In addition to the above, the proposed results corroborate with the fact that the sheath-structure is closely related with ion-acoustic shock formation and evolution. The sheath, in fact, if travelling through the plasma, would depict shock wave propagation, notwithstanding dissimilar boundary conditions. In this context, the formation of non-monotonic double layer structures developed by the coupling of the non-neutral monotonic Debye sheath and the charged body boundary of the plasma-confining wall is noteworthy [27]. Thus, an alternative sheath-based viewpoint on igniting hydrodynamic shocks is speculated. Lastly, it is conceded that the proposed analysis relies on the approximation of two distinct isothermal magnetized fluids (electronic plus ionic) for the sake of simplicity. But, recent hydro-kinetic studies have shown that the ion temperature may change appreciably (with varying adiabaticity) over the plasma wall-transition layer [28, 29]. It indicates that further refinements are indeed needed for a more profound exploration of the plasma boundary-wall interaction processes.

REFERENCES

[1] Ahedo, E. Structure of the plasma-wall interaction in an oblique magnetic field. *Physics of Plasmas*, 4:4419-4430, 1997.

[2] Bohm, D. *The Characteristics of Electrical Discharges in Magnetic Fields*. edited by Guthrie, A., Wakerling, R. McGraw-Hill, New York, 1949.

[3] Alterkop, B., Goldsmith, S., and Boxman, R. L. Presheath in fully ionized collisional plasma in a magnetic field. *Contribution to Plasma Physics*, 45:485-493, 2005.

[4] Riemann, K. U., Seebacher, J., Tskhakaya Sr., D. D., and Kuhn, S. The plasma-sheath matching problem. *Plasma Physics and Controlled Fusion*, 47:1949-1970, 2005.

[5] Franklin, R. N. The plasma-sheath boundary region. *Journal of Physics D: Applied Physics*, 36:R309-R320, 2003.

[6] Langmuir, I. The interaction of electron and positive ion space charges in cathode sheaths. *Physical Review*, 33:954-989, 1929.

[7] Riemann, K. U. The influence of collisions on the plasma sheath transition. *Physics of Plasmas*, 4:4158-4166, 1997.

[8] Deka, U. and Dwivedi, C. B. Effect of electron inertial delay on Debye sheath formation. *Brazilian Journal of Physics*, 40(3):333-339, 2010.

[9] Severn, G. D. A note on the plasma sheath and the Bohm criterion. *American Journal of Physics*, 75:92-94, 2007.

[10] Karmakar, P. K., Deka, U., and Dwivedi, C. B. Graphical analysis of electron inertia induced acoustic instability. *Physics of Plasmas*, 12:032105(1-9), 2005.

[11] Karmakar, P. K., Deka, U., and Dwivedi, C. B. Response to "Comment on 'Graphical analysis of electron inertia induced acoustic instability'". *Physics of Plasmas*, 13:104702(1-3), 2006.

[12] Deka, U., Dwivedi, C. B., and Ramachandran, H. Propagation of ion-acoustic wave in the presheath region of a plasma sheath system. *Physica Scripta*, 73:87-97, 2006.

[13] Schmitz, H., Riemann, K. U., and Daube Th. Theory of the collisional presheath in a magnetic field parallel to the wall. *Physics of Plasmas*, 3:2486-2495, 1996.

[14] Stangeby, P. C. The Bohm-Chodura plasma sheath criterion. *Physics of Plasmas*, 2:702-706, 1995.

[15] Zou, X., Liu, J. Y., Gong, Y., Wang, Z-X., Liu, Y., and Wang, X-G. Plasma sheath in a magnetic field. *Vacuum*, 73:681-685, 2004.

[16] Allen, J. E. The plasma boundary in a magnetic field. *Contribution to Plasma Physics*, 48:400-405, 2008.

[17] Hatami, M. M. The properties of the space-charge and net current density in magnetized plasmas. *Plasma Science and Technology*, 15(12):1169-1173, 2013.

[18] Zou, X., Qiu, M., Liu, H., Zhang, L., Liu, J., and Gong, Y. The ion density distribution in a magnetized plasma sheath. *Vacuum*, 83:205-208, 2009.

[19] Liu, H., Zou, X., and Qiu, M. Sheath criterion for an electronegative plasma sheath in an oblique magnetic field. *Plasma Science and Technology*, 16(7):633-636, 2014.

[20] Ou, J. and Yang, J. Properties of a warm plasma collisional sheath in an oblique magnetic field. *Physics of Plasmas*, 19:113504(1-7), 2012.

[21] Riemann, K. U. The Bohm criterion and sheath formation. *Journal of Physics D: Applied Physics*, 24:493-518, 1991.

[22] Rohde, U. L., Jain, G. C., Poddar, A. K., and Ghosh, A. K. *Introduction to Integral Calculus*. Wiley, New Jersey, 2012.

[23] Khoramabadi, M., Ghomi, H. R., and Ghoranneviss, M. Effects of ion temperature on collisional DC sheath in plasma ion implantation. *Journal of Plasma and Fusion Research SERIES*, 8:1399-1402, 2009.

[24] Ghomi, H. and Khoramabadi, M. Influence of ion temperature on plasma sheath transition. *Journal of Plasma Physics*, 76:247-255, 2010.

[25] Butcher, J. C. An introduction to "Almost Runge-Kutta" methods. *Applied Numerical Mathematics*, 24:331-342, 1997.

[26] Khoramabadi, M., Ghomi, H., and Ghoranneviss, M. Ion temperature effects on magnetized DC plasma sheath. In Proceedings of the 19th International Plasma Chemistry Society (ISPC-19), 5-10 July 2009, Germany.

[27] Alterkop, B. A., Dubinova, I. D., and Dubinov, A. E. Structure of the charged sheath at the plasma-charged body boundary. *Journal of Experimental and Theoretical Physics*, 102:173-181, 2006.

[28] Kuhn, S., Riemann, K. U., Jelic, N., Tskhakaya Sr., D. D., Tskhakaya Jr., D., and Stanojevic, M. Link between fluid and kinetic parameters near the plasma boundary. *Physics of Plasmas*, 13:013503(1-8), 2006.

[29] Robertson, S. Sheaths in laboratory and space plasmas. *Plasma Physics and Controlled Fusion*, 55:093001(1-34), 2013.